Homology Modeling, Molecular Dynamics and Inhibitor Binding Study on MurD Ligase of Mycobacterium Tuberculosis

ARTICLE *in* INTERDISCIPLINARY SCIENCES COMPUTATIONAL LIFE SCIENCES · SEPTEMBER 2012

Impact Factor: 0.66 · DOI: 10.1007/s12539-012-0133-x · Source: PubMed

Vivek Kumar

Parameswaran Saravanan
Anna University, Chennai

Gopi Mohan
Amrita Institute of Medical Sciences and Res…

Interdiscip Sci Comput Life Sci (2012) 4: 223–238
DOI: 10.1007/s12539-012-0133-x

Homology Modeling, Molecular Dynamics and Inhibitor Binding Study on MurD Ligase of *Mycobacterium Tuberculosis*

Akanksha ARVIND[1†], Vivek KUMAR[1], Parameswaran SARAVANAN[2], C. Gopi MOHAN[3*]
[1](Department of Pharmacoinformatics, National Institute of Pharmaceutical Education and Research (NIPER), S.A.S. Nagar, Punjab 160062, India)
[2](Department of Biochemistry, Indian Institute of Technology, Guwahati, Assam 781039, India)
[3](Amrita Centre for Nanosciences and Molecular Medicine (ACNSMM), Amrita Institute of Medical Sciences & Research Centre, Amrita Vishwa Vidyapeetham University, Ponekkara, Kochi 682041, Kerala State, India)

Received 12 October 2011 / Revised 21 March 2012 / Accepted 6 July 2012

Abstract: The cell wall of mycobacterium offers well validated targets which can be exploited for discovery of new lead compounds. MurC-MurF ligases catalyze a series of irreversible steps in the biosynthesis of peptidoglycan precursor, *i.e.* MurD catalyzes the ligation of D-glutamate to the nucleotide precursor UMA. The three dimensional structure of *Mtb*-MurD is not known and was predicted by us for the first time using comparative homology modeling technique. The accuracy and stability of the predicted *Mtb*-MurD structure was validated using Procheck and molecular dynamics simulation. Key interactions in *Mtb*-MurD were studied using docking analysis of available transition state inhibitors of *E.coli*-MurD. The docking analysis revealed that analogues of both L and D forms of glutamic acid have similar interaction profiles with *Mtb*-MurD. Further, residues His192, Arg382, Ser463, and Tyr470 are proposed to be important for inhibitor-(*Mtb*-MurD) interactions. We also identified few pharmacophoric features essential for *Mtb*-MurD ligase inhibitory activity and which can further been utilized for the discovery of putative antitubercular chemotherapy.
Key words: *Mtb*-MurD, homology modeling, molecular dynamics, molecular docking, chemotherapy, peptidoglycan, resistance, protein structure.
Abbreviations: TB, tuberculosis; *Mtb*, *Mycobacterium tuberculosis*; MurD, UDP-*N*-acetylmuramoyl-*L*-alanine-D-glutamate ligase; UMA, UDP-N-acetylmuramoyl-L-alanine; DOTS, directly observed treatment short course; WHO, World Health Organization; D-Glu, D-glutamate; UMAG, UDP-*N*-acetylmuramoyl-L-alanine-D-glutamate; MD, molecular dynamics.

1 Introduction

Infectious diseases were thought to be conquered with the arrival of antibiotics, but irrational use of antibiotics particularly in developing countries has lead to the emergence of its resistance. TB is an infectious disease caused by *Mtb* and is a serious public health threat worldwide particularly in immuno-compromised patients. It is the second leading infectious killer next only to HIV and takes toll of millions of lives annually (Tuberculosis facts, 2011/2012). Although, the recent emergence of drug resistant strains of *Mtb* has stimulated research for newer and more potent molecular target for inhibiting tubercle bacilli growth (Cole *et al.*, 1998). Moreover, *mycobacteria* are rod shaped facultative aerobe which survives best at high oxygen tension and alkaline pH. Further, it gets colonized in the pulmonary walls leading to the high occurrence of pulmonary TB (Parish *et al.*, 1999).

Global alliance for TB drug development was established in 2000, with the aim of providing high quality diagnosis and treatment to all patients in a cost effective manner. The DOTS strategy for the treatment of TB was initiated by WHO and has proven to be the most successful and cost effective measure to combat TB (Raviglione *et al.*, 2002; Murray *et al.*, 1990). This strategy includes standardized combinations of first line drugs given under direct observation, which include ethambutol, streptomycin, rifampicin, isoniazid and pyrazinamide. However, this strategy also has side effects such as hepatotoxicity, pheripheral neuritis, hyperuricemia, enzyme induction and development of resistance. Several other factors like patient incom-

†Present address: Department of Medicinal Chemistry, University of Illinois at Chicago, 833 S Wood Street, Chicago IL 60612, USA.
*Corresponding author.
E-mail: cgopimohan@yahoo.com

patibility due to long periods of treatment, incompatibility with antiretrovirals questions the effectiveness of the therapy. Moreover, no new drug came in the market since last 40 years which makes the TB treatment more cumbersome (Khasnobis *et al.*, 2002). However, several chemical compounds belonging to novel classes have been subjected to extensive *in vitro* screening for their antimycobacterial activity. These novel classes include fluroquinolones, macrolides, oxazolidinones, and nitroimidazoles, pyrroles, pleuromutilins, and diarylquinolines (Spigelman *et al.*, 2007). While, in order to address the problem of drug resistance, new potential targets need to be discovered. With the availability of *Mtb* genome, a vast target space has opened up. More than 400 targets are under investigation in TB structural genomics consortium. 185 out of these 400 targets were identified by comparative metabolic analysis and many of those are under various phases of investigation (Anishellty *et al.*, 2005).

The cell wall of mycobacteria is an excellent starting point for designing of antimycobacterial drug, as the most prescribed drugs like isoniazid and ethambutol acts by inhibiting the cell wall synthesis. Many antibacterial agents like bacitracin, vancomycin, penicillins and cephalosporins, act by inhibiting the late enzymatic steps of bacterial peptidoglycan biosynthesis, whereas the early intracellular steps catalyzed by a series of Mur enzymes (MurA, MurB, MurC, MurD, MurE and MurF) has been unexploited as antibacterial targets.

MurD is an important target involved in cell wall biosynthesis. It has a molecular weight of 49.3 kDa, and expressed in cytoplasm as a single chain monomer of 486 amino acids length. It belongs to Mur CDEF ligase family. *Mtb*-MurD is enzymatically/structurally similar to MurD of *E. coli* (1EEH, 1UAG and 2JFF) (Crick *et al.*, 2001) with a protein sequence identity of 31% and similarity of 45% respectively. It catalyzes the peptide bond formation reaction between UMA and D-Glu (EI Zoeiby *et al.*, 2003). The catalytic mechanism of MurD is well established. Initially, MurD catalyzes the ATP dependent phosphorylation of carboxylic acid of UMA. The resulting acyl-phosphate is then attacked by the incoming D-Glu to form a high-energy tetrahedral intermediate, which finally collapses into the amide product, UMAG and inorganic phosphate. This mechanism is central to all amide ligases family including Mur ligases which are confirmed by X-ray diffraction analysis (Bertrand *et al.*, 1999), isotope transfer (Falk *et al.*, 1996) and rapid quench experiment (Emanuele *et al.*, 1997). Moreover, *Mtb*-MurD has been suggested as a broad spectrum target for designing antibacterial drugs (White *et al.*, 2004) and is also essential for the survival of *Mtb* (Zhang *et al.*, 2004).

MurD ligase has three binding sites - substrate binding site, ATP binding pocket and glutamic acid binding site. The key residues which are involved in the substrate binding in *E. coli*-MurD are Leu15, Thr16, Thr36, Arg37, Gly73, Asn138, Gln162 and His183 (corresponding residues in *Mtb*-MurD ligase are Val18, Thr19, Asp39, Asp40, Gly75, Asn147, Gln171 and His192) (Bertrand *et al.*, 1999) respectively. Similarly, the residues for the ATP binding in *E. coli*-MurD are Gly114, Lys115, Ser116, Thr117, Glu157, Asn271, Arg302 and Asp317 (corresponding residues in *Mtb*-MurD ligase are Gly123, Lys124, Thr125, Thr126, Glu166, Asp283 and Arg314) respectively. Finally, residues involved in glutamic acid binding pocket are Lys348, Ser415 and Phe422 (corresponding residues in *Mtb*-MurD ligase are Arg382, Ser463 and Tyr470) respectively (Kotnik *et al.*, 2007). Using site-directed mutagenesis analysis by Bouhss *et al.* it was shown that His183Ala mutant showed dramatic decrease in UMA binding affinity in *E. coli*-*Mtb* ligase (Bouhss *et al.*, 1999).

2 Materials and methods

All computational experiments were carried out using Modeller9v4, GLIDE, Gromacs3.3.3 and SYBYL7.1 molecular modeling packages on Sun workstation with Red Hat Enterprise Linux 3 and Silicon Graphics Fuel Workstation with IRIX 6.5 operating system.

2.1 Homology modeling

Modeller9v4 program was used to build three-dimensional (3D) structural model of the MurD ligase of *Mtb* (Martí-Renom *et al.*, 2000).Modeller is a computer program that models 3-D structures of proteins and their assemblies by satisfaction of spatial restraints. The amino acid sequence of *Mtb*-MurD ligase was retrieved from SwissProtKB/TrEMBL database (id: O06222) (Boeckmann *et al.*, 2003). NCBI-BLASTP search was carried out against Protein Data Bank (PDB) (Bernstein *et al.*, 1977) using *Mtb*-MurD ligase as query sequence, and the number of homologous sequences was retrieved. Among these sequences, 2JFH (crystal structure of *E. coli*-MurD ligase in complex with L-Glu containing sulfonamide inhibitor) was selected as the best template to build *Mtb*-MurD ligase homology model.

The primary sequence alignment of template-(*Mtb*-MurD) was done using ClustalW1.83 (Chenna *et al.*, 2003) program, and is shown in Fig. 1. This alignment was then used to produce 3D model of *Mtb*-MurD ligase using Modeller9v4. The crude models were then refined on the basis of DOPE and molpdf scores followed by analysis of various stereo-chemical parameters like Ramachandran, ERRAT plot, RMSD comparison and molecular dynamics simulations (Kumar *et al.*, 2010).

2.2 Molecular dynamics simulations study

MD stimulations were carried out using 43A1 force field of Gromacs96 implemented in the GROMACS

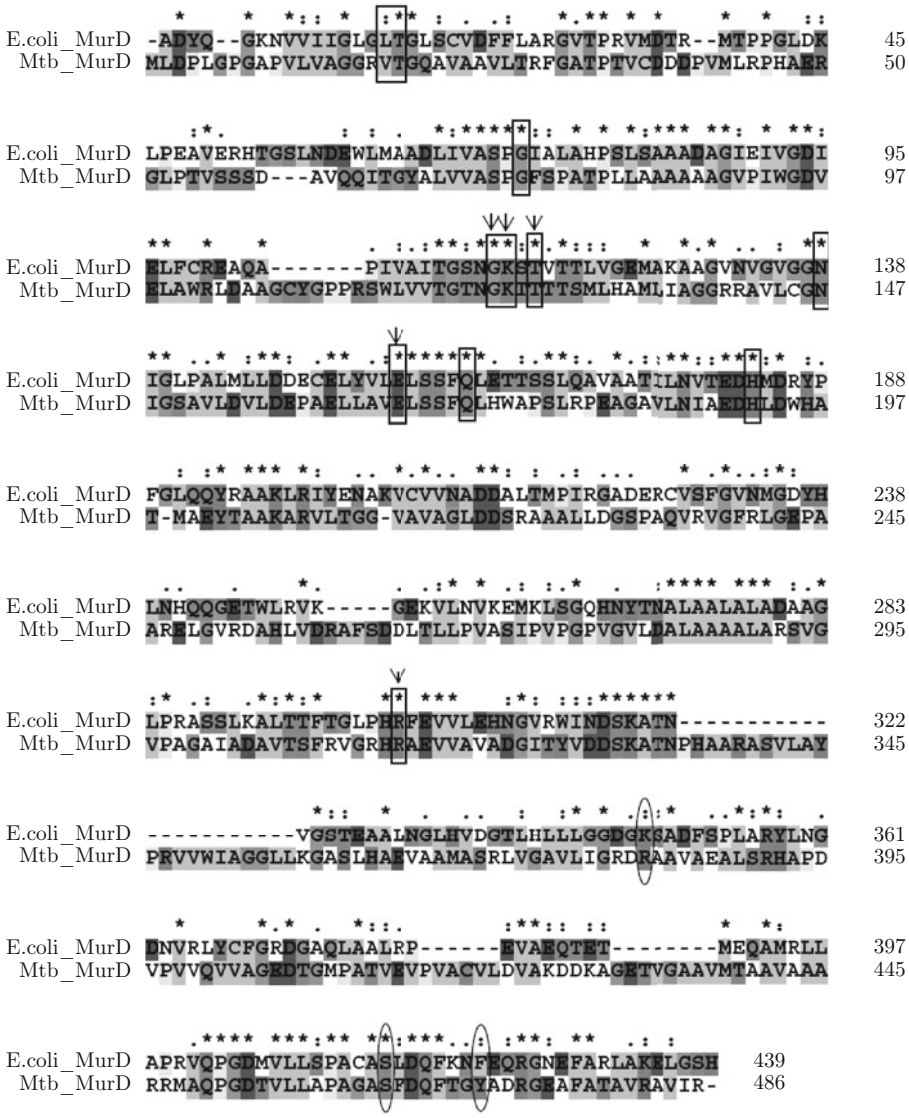

Fig. 1 Pairwise sequence alignment of *Mtb*-MurD ligase with *E. coli*-MurD (2JFH). Stars indicate identical amino acids while double and single dot for similarity of amino acid with respect to its property. Rectangle boxes indicate conserved amino acid at the ligand binding residue while oval and rectangle box with arrow indicate conserved residues at glutamic acid and ATP binding pocket respectively.

(Lindahl *et al.*, 2001) software package. A cubic box with the SPC water model was built and submitted to maximum 1000 steps of energy minimization using the steepest descent gradient algorithm. Leap-frog algorithm was used for integrating Newton's equations in MD simulation. *Mtb*-MurD ligase complex with the inhibitor N-(6-butoxy-naphthalene-2-sulfonyl)-L-glutamic acid was subjected to equilibration for 1000 steps. All heavy atoms of *Mtb*-MurD were restrained, leaving water and ligand to interact with the protein. It is followed by a full MD simulation of 4 ns at 300 K, using 2 fs step integration time. Constraints were used on all protein covalent bonds to maintain the constant bond length. Berendsen temperature and Parinello-Rahman pressure coupling were used to subdue the drift effect during equilibration and MD simulation. Co-ordinates and energy terms (potential energy for the whole system) were saved for every 10000 steps, with the aim of evaluating the protein system stabilization throughout MD simulations.

2.3 Molecular docking study

All inhibitors along with their half maximal inhibitory concentration (IC_{50}) value or residual activity (RA) in % and molecular structures are presented in Table 1. The IC_{50} value is a measure of the efficacy of a chemical/biological compound and its quantitative value generally indicates how much concentration of a particular drug is needed to inhibit 50% of a given biological/biochemical process (Neubig *et al.*, 2003). The transition state inhibitors were docked at the active

Table 1 Compounds with their biological activity (IC_{50} or RA) and docking score

Comp. No.	Structure	[a]IC_{50} (μM)/ [b]RA (%)	Glide Docking Score	Residues Involved in H-bonding Interactions
	Phosphinate Series			
12g	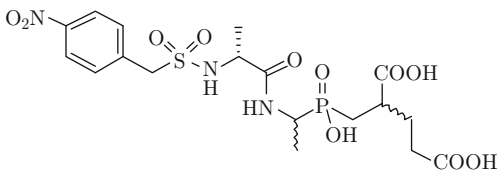	78	−8.03	Ser463, Arg382, Tyr470
12c	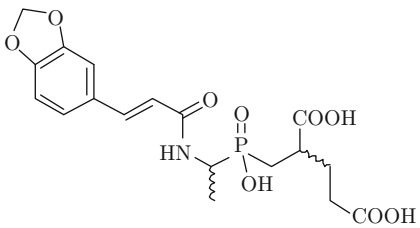	95	−7.69	Ser463, Arg382, Tyr470, His192, Arg17
12f	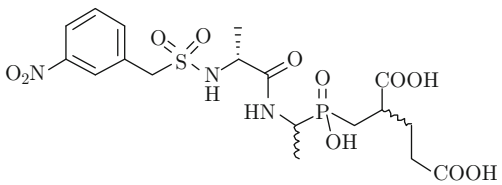	19%	−7.43	Ser463, Arg382, His192, Arg17, Gly75
13i	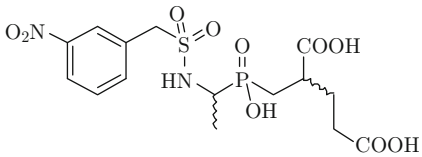	22%	−7.20	Ser463, Arg382, Tyr470, His192, Gly16
12b	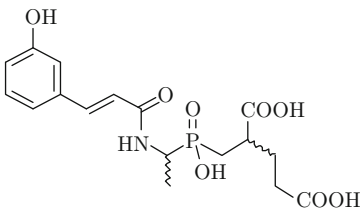	23%	−7.45	Ser463, Arg382, Tyr470, Arg17
12a	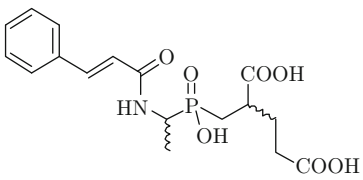	432	−7.24	Ser463, Arg382, Tyr470, Thr333
13h	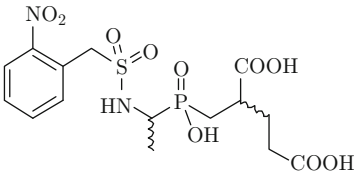	30%	−7.05	Ser463, Arg382, Tyr470, Arg17

Continued

Comp. No.	Structure	[a]IC_{50} (μM)/ [b]RA (%)	Glide Docking Score	Residues Involved in H-bonding Interactions
12d	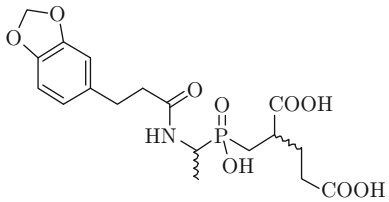	36%	−7.60	Ser463, Arg382, Tyr470, Arg17
13g	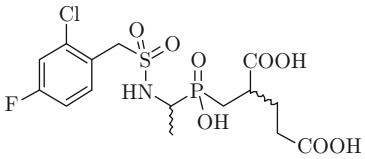	37%	−7.33	Ser463, Arg382, Tyr470
13d	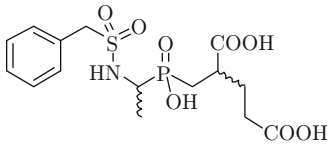	40%	−6.82	Ser463, Arg382, Tyr470, His192, Arg17, Gly75
8a	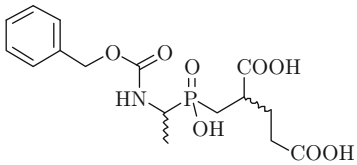	41%	−6.90	Ser463, Arg382, Tyr470, His192
12e	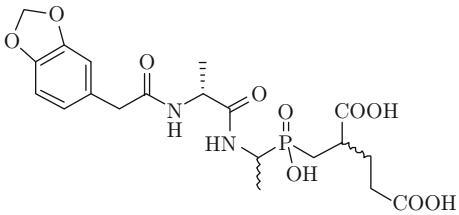	44%	−7.75	Ser463, Arg382, Tyr470, His192, Gly75
13j	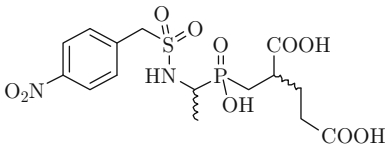	47%	−6.97	Ser463, Arg382, Tyr470, His192
13e	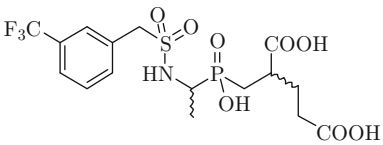	49%	−7.20	Ser463, Arg382, Tyr470, His192, Gly16

Continued

Comp. No.	Structure	[a]IC_{50} (μM)/ [b]RA (%)	Glide Docking Score	Residues Involved in H-bonding Interactions
13f	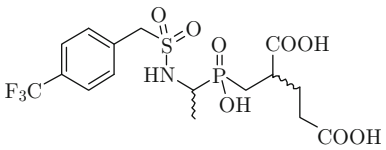	50%	−7.38	Ser463, Arg382, Tyr470, His192
13b	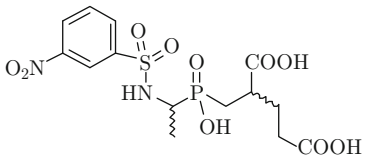	52%	−6.87	Ser463, Arg382, Tyr470, Asp191
13a	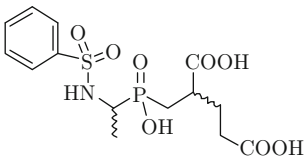	54%	−6.67	Ser463, Arg382, Tyr470
13c	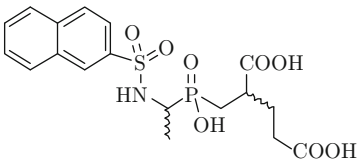	55%	−7.44	Ser463, Arg382, Tyr470, His192
15	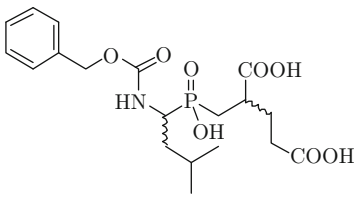	65%	−7.34	Ser463, Arg382, Tyr470, His192, Thr333
14	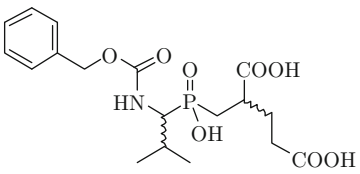	66%	−7.06	Ser463, Arg382, Tyr470
16	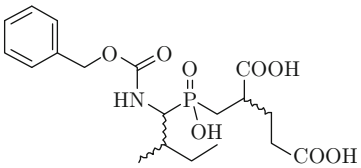	83%	−7.28	Ser463, Arg382, Tyr470, Thr333

Continued

Comp. No.	Structure	[a]IC_{50} (μM)/ [b]RA (%)	Glide Docking Score	Residues Involved in H-bonding Interactions
21	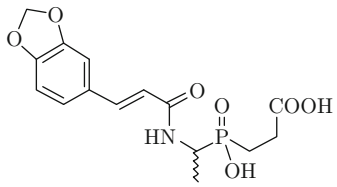	91%	−4.83	Ser463, Arg382, Tyr470, His192
23	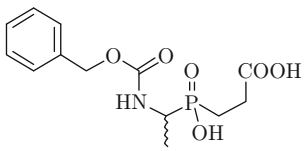	92%	−4.83	Ser463, Arg382, Tyr470, His192
22	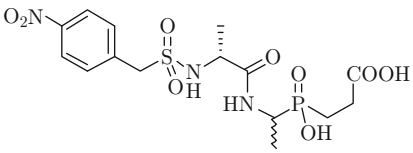	100%	−5.45	Ser463, Arg382, His192, Gly16
Naphthalene-*N*-sulfonyl-D-glutamic acid series				
17k	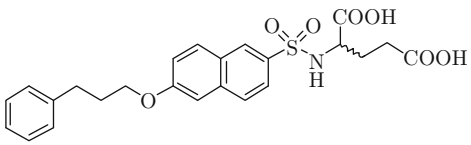	132	−8.74	Ser463, Tyr470, Arg382, His192
17d	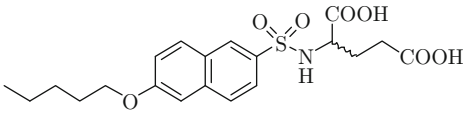	170	−8.69	Ser463, Tyr470, Arg382, His192, Arg17
38	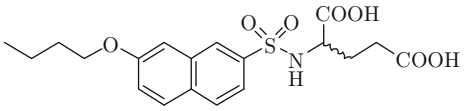	180	−8.64	Ser463, Tyr470, Arg382, His192, Arg17
17c	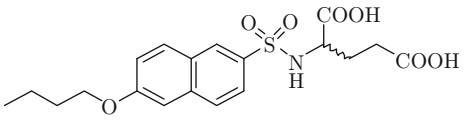	280	−8.51	Ser463, Tyr470, Arg382, His192, Arg17

Continued

Comp. No.	Structure	[a]IC_{50} (μM)/ [b]RA (%)	Glide Docking Score	Residues Involved in H-bonding Interactions
17a	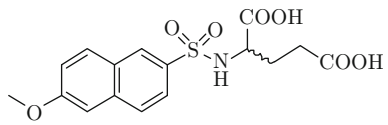	590	−8.36	Ser463, Tyr470, Arg382, His192, Arg17
17o	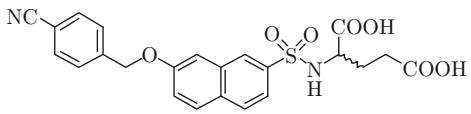	122	−8.33	Ser463, Tyr470, Arg382, His192, Gly16
17f	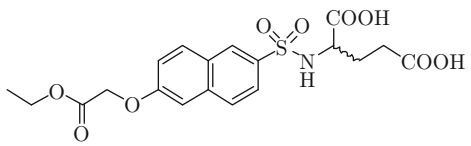	192	−8.27	Ser463, Tyr470, Arg382, His192, Arg17
17l	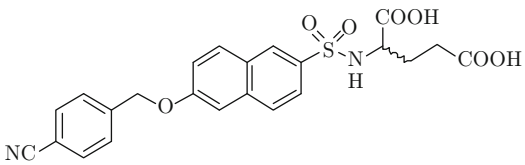	105	−8.13	Ser463, Tyr470, Arg382, His192
17g	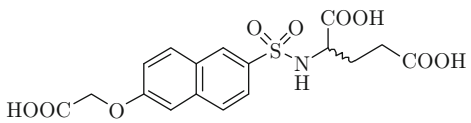	630	−8.08	Ser463, Tyr470, Arg382, His192, Gly16
17h	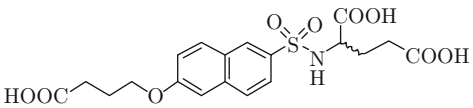	> 1000	−8.07	Ser463, Tyr470, Arg382, His192, Thr333, Gly16, Asp39
17e	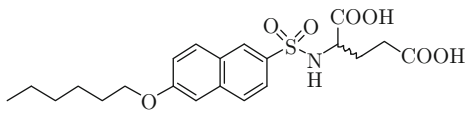	176	−7.90	Ser463, Tyr470, Arg382, His192

Continued

Comp. No.	Structure	[a]IC_{50} (μM)/ [b]RA (%)	Glide Docking Score	Residues Involved in H-bonding Interactions
26	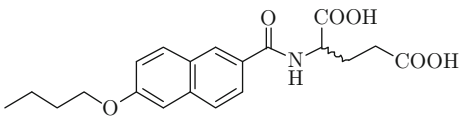	1000	−7.84	Ser463, Tyr470, Arg382, His192
11d	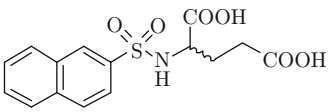	810	−7.82	Ser463, Tyr470, Arg382, His192
12	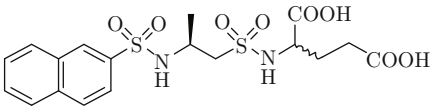	2000	−7.72	Ser463, Tyr470, Arg382, His192
17b	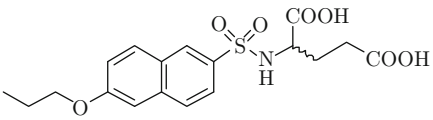	305	−7.68	Ser463(2), Tyr470, Arg382(2), His192
39	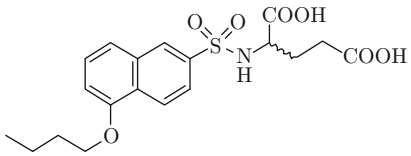	> 1000	−7.67	Ser463, Tyr470, Arg382, His192
11c	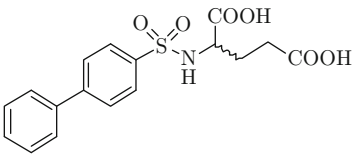	1720	−7.52	Ser463, Tyr470, Arg382, His192
17n	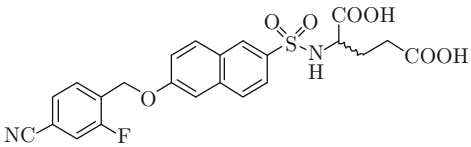	85	−7.50	Ser463, Arg382, Tyr470, His192

Continued

Comp. No.	Structure	[a]IC_{50} (μM)/ [b]RA (%)	Glide Docking Score	Residues Involved in H-bonding Interactions
17i	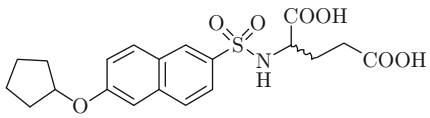	400	−7.37	Ser463, Arg382, Tyr470, His192
17j	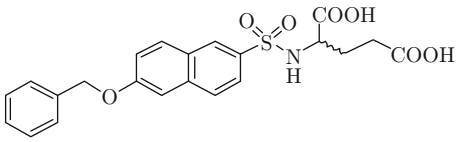	239	−7.17	Ser463, Arg382, Tyr470, His192
17m	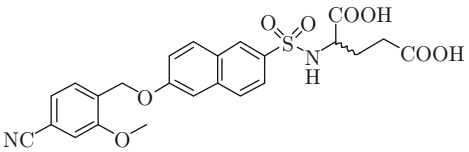	100	−7.11	Ser463, Arg382, His192
40	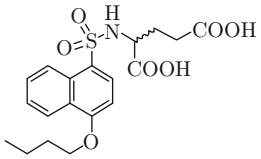	> 1000	−6.82	Ser463, Tyr470, Arg382, His192, Thr333
31	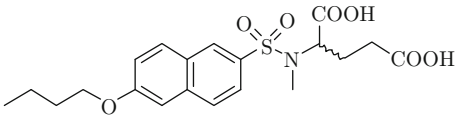	> 1000	−6.74	Ser463, Arg382, His192
29	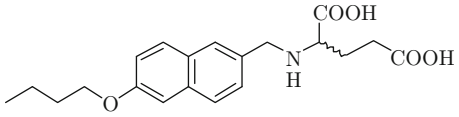	> 1000	−6.55	Ser463, Tyr470, Arg382, His192
18	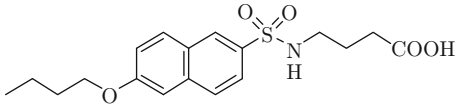	> 2000	−4.89	Ser463, Arg382, His192

Continued

Comp. No.	Structure	[a]IC_{50} (μM)/ [b]RA (%)	Glide Docking Score	Residues Involved in H-bonding Interactions
19	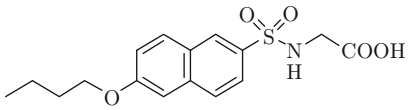	> 2000	−4.82	Ser463, Tyr470, Arg382, His192
16c	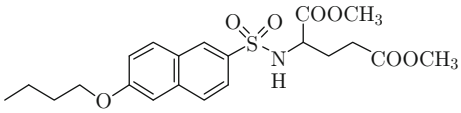	> 2000	−3.80	Tyr470, Arg382

[a]IC_{50} value signifies the 50% inhibition of enzymatic activity at particular concentration of the chemical compound.
[b]RA signifies the % residual activity of the compound for 1 mM inhibitory concentration.

site of the *Mtb*-MurD ligase with the aim to determine its binding mode with the different inhibitors. Two series of transition state inhibitors viz. naphthalene-N-sulfonyl-D-glutamic acid derivatives (Humljan *et al.*, 2008) and phosphinate inhibitors (Štrancar *et al.*, 2006) were chosen from the literature to perform molecular docking study in order to explore their binding mode at the active site. The inhibitors were sketched and minimized by conjugate gradient method using Tripos force field with 0.05 kcal/mol energy gradient convergence criterion implemented in Sybyl7.1 program. The molecular docking program, GLIDE (Grid-based Ligand Docking with Energetics) was used for docking and binding analysis (Schrödinger, 2007). Glide algorithm is based on a systematic search of positions, orientations, and conformations of the ligand in the receptor binding site using funnel type approach. 20 poses per ligand were allowed to generate on completion of each docking calculations (Friesner *et al.*, 2004) and were further prioritized using the docking score (Eldridge *et al.*, 1997).

Mtb-MurD protein model was prepared for the docking studies using the Protein Preparation Wizard tool implemented in Maestro. Restrained minimization of *Mtb*-MurB model was performed using *Impref utility* by applying constraints to all the heavy atoms in the protein model, until the RMSD of the hydrogen atoms reached 0.30 Å. An interaction grid of 10 Å was generated for *Mtb*-MurD protein model by using the receptor grid generation module of Glide, and taking bound inhibitor as the reference for docking study. The grid was prepared by positioning its center on the bound ligand in the protein structure by using centroid for the grid generation. The grid box was extended 10 Å from the center, with the outer box extending an additional 27.9 Å covering the active site cavity. The coordinates of the enclosing boxes were: x = 20.89 Å; y = −2.69 Å; z = 19.96 Å respectively.

All ligands in the present study along with **17c-o** (extracted from co-crystal structures; PDB id: **2UUO**, **2UUP**, **2VTD** and **2VTE)** were prepared using LigPrep wizard of Glide by generating low energy ionization, tautomeric and stereoisomeric states within the range of pH 7.0 ± 2.0 using OPLS force field. Structures obtained from LigPrep wizard were docked into the binding site of the homology model of *Mtb*-MurD using the set protocol in Glide at the standard precision mode. Poses which are closest to the bound ligand in protein structure were selected for the analysis and their docking scores are reported.

3 Results and discussion

3.1 Homology modeling

E. coli-MurD (PDB code: 2JFH) primary sequence, a top hit from BLAST search was selected as template for homology modeling of *Mtb*-MurD ligase. It has 31% sequence identity and 45% sequence similarity with the query sequence (Fig. 1). The final model of *Mtb*-MurD ligase obtained after refinement and energy minimization was validated with Ramachandran plot, ERRAT plot, RMSD comparison and MD simulations (Figs. S1-S3). The final *Mtb*-MurD ligase model with the ligand is depicted in Fig. 2. *Mtb*-MurD ligase has three domains viz. N-terminal domain, central domain and C-terminal domain respectively. All three domains belong to alpha and beta (α/β) class. N-terminal domain (1-94) comprised of one β sheet of four parallel β strands and three α helices arranged in two layered $\beta-\alpha-\beta$ units to give rise to an incomplete Rossmann like fold. The overall

domain depicted the NADH-binding Rossmann like domain. The central domain (95-307) was comprised of two β sheets of six and three β strands and total ten α helices arranged in three layered $\alpha - \beta - \alpha$ units. Furthermore, the 8th strand was anti-parallel to rest of the strands and the overall fold resembled to ribokinase fold. The C-domain (308-486) comprised of one β sheet containing six β strands, in which the first β strand is anti-parallel to rest of the strands and total six α helices were present. The overall fold resembled the peptide binding domain which was specific to Mur CDEF family and denoted as MurD-like peptide ligase fold.

Ramachandran plot of *Mtb*-MurD ligase model revealed 89.1% amino acid residues in the core region, 8.9% in the allowed region and 2.0% in the generously allowed region respectively. Moreover, none of the residues was observed in the disallowed region (Fig. S1). Thus, our *Mtb*-MurD ligase model is stereo chemically significant with the reasonable distribution of backbone angle in the protein structure and acceptability of the built model. The ERRAT plot depicted the various non-bonded interactions between different atom types of amino acid. It provided the structure modifying guidance to improve the sterically hindered regions in the protein. The overall quality factor of homology model was 94.8% in ERRAT plot, which further enhanced the confidence of accepting the *Mtb*-MurD ligase model (Fig. S2). *E. coli*-MurD and *Mtb*-MurD ligase model in region of 6 Å, 8 Å and 10 Å around the inhibitor (N-[(6-butoxynaphthalen-2-yl) sulfonyl]-L-glutamic acid) was superimposed and compared to analyze the structural drift. The RMSD values were observed below 0.5 Å for all the above mentioned regions (Table 2). It further emphasized over the quality of the built model due to the minimum deviation with respect to backbones and side chains (Fig. 2) respectively.

Table 2 RMSD values at different regions around the ligand of *E. coli*-MurD and Mtb-MurD ligase

Regions aligned	RMSD values 6 Å region around ligand (Å)	RMSD values 8 Å region around ligand (Å)	RMSD values 10 Å region around ligand (Å)
C-alpha	0.13	0.72	0.86
Backbone	0.30	0.71	0.87
Side chain	1.18	1.47	1.86
All	0.84	1.14	1.41

3.2 Molecular dynamics simulations

MD simulations were performed to determine the stability of the predicted 3D structure of *Mtb*-MurD ligase. The trajectory was stable during the whole production phase of the 4 ns MD run. It was generally monitored and confirmed by the analysis of backbone RMSD and the potential energy as a function of time for the *Mtb*-MurD ligase (Fig. 3). RMSD values for the *Mtb*-MurD showed a rise in the first 1500 ps and then remained stable for rest of the simulation time. The average RMSD for the *Mtb*-MurB model was found to be 0.37 nm, while the potential energy remained stable throughout the MD simulation (Fig. 3). Three hydrogen bonding interactions were observed to stabilize the (*Mtb*-MurD)-ligand complexes (Fig. S3a). These facts were also verified by the docking study, where probably three residues viz. Ser463, Tyr470 and His192 or Ser382 were found to make strong hydrogen bonding interactions with the ligand. It was noticed that throughout the MD simulations of *Mtb*-MurD, very few fluctuations exceeded ≥ 0.2 nm and even less fluctuations passed over ≥ 0.3 nm respectively (Fig. S3b). However, the flexibility was quite negligible (0.2 nm); although graph showed residues at the N-terminal, 250–260 and 325–385 were slightly more flexible and had fluctuations close to 0.3 nm, while the active site residues remained stable throughout 4 ns MD simulations.

3.3 Molecular docking analysis

Docking analysis was performed on 51 *Mtb*-MurD inhibitors to identify key amino acid residues involved in making interactions with the *Mtb*-MurD model structure. The structure of all *Mtb*-MurD inhibitors, their experimental activity (IC_{50}) and Glide-computed docking score along with the H-bond interacting residues are presented in Table 1. *Mtb*-MurD inhibitors belong to two different chemical classes-phosphinate and naphthalene-*N*-sulfonyl-D-glutamic acid. All inhibitors were docked in the active site of the *Mtb*-MurD homology model, showing good docking scores. The distance and angle cut-off considered for hydrogen bonding interactions were: (a) distance between proton donor and acceptor atom was ≤ 3.5 Å, and (b) the angle between donor-H…acceptor was $\geq 120°$. The compounds from both series exhibited the probable hydrogen bonding interactions with Arg382, Ser463 and Tyr470 residues respectively. Further, all naphthalene-*N*−sulfonyl-D-glutamic acid derivatives, and twelve out of twenty four compounds from phosphinate series displayed hydrogen bonding interactions with His192, suggesting its key role in inhibitor binding.

Generally, *Mtb*-MurD inhibitors exist in isomeric forms and speculated to interact in a similar manner at the active site of the *Mtb*-MurD. The L- and D-glutamic acid isomers of compound **17k** belonging to naphthalene-*N*-sulfonyl-D-glutamic acid series were docked in the homology model of *Mtb*-MurD to verify its mechanism of interactions. The compound **17k** has

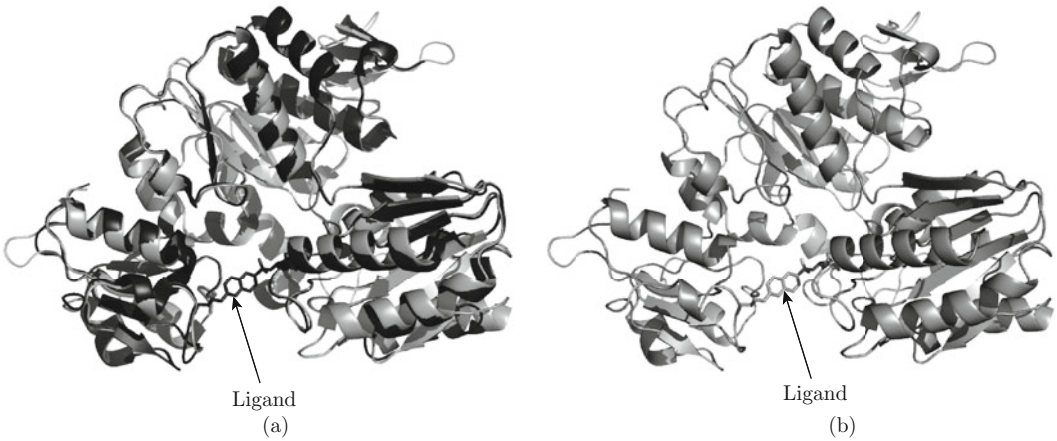

Fig. 2 (a) Superimposition of *E. coli*-MurD (black) and Mtb-MurD ligase (gray). (b) Homology model of Mtb-MurD ligase with ligand N-[(6-butoxynaphthalen-2-yl) sulfonyl]-L-glutamic acid shown in ball and stick model.

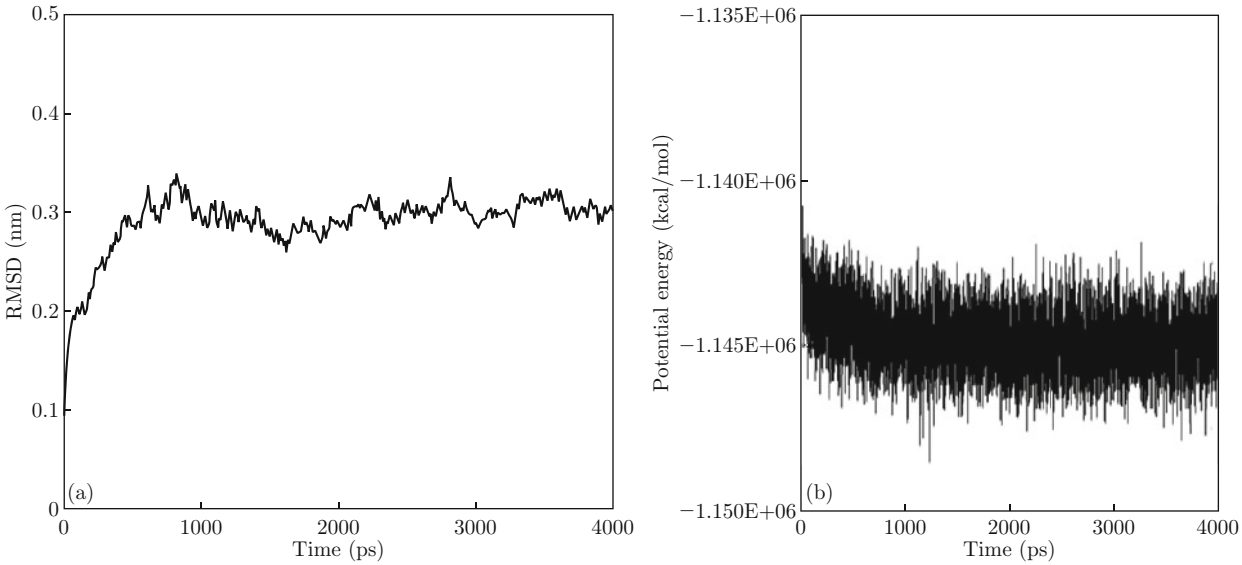

Fig. 3 Graphical representation of RMSD of back bone carbons from starting structure of Mtb-MurD model as a function of time (a) and plot of potential energy vs. simulation time (b).

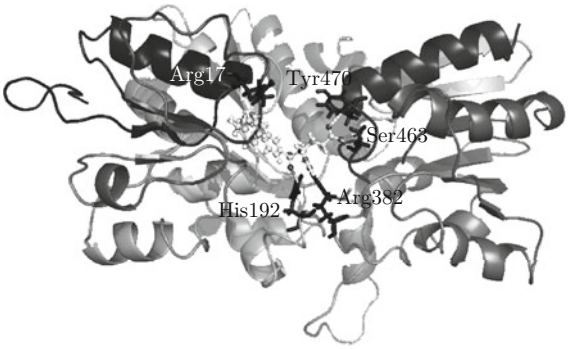

Fig. 4 Compound **17k** docked in the active site of *Mtb*-MurD ligase model. Residues involved in hydrogen bonding were shown in stick and hydrogen bonds are shown as dotted lines.

highest binding affinity in terms of docking score and showed hydrogen bonding interaction with the residues Arg17, Arg382, Ser463, Tyr470 and His192 (Figs. 4 & 5) respectively.

The docked poses of different isomeric forms have minor difference of docking scores ∼0.4. The interaction pattern of these two isomeric forms were observed similar, as the carboxylic groups of glutamic acid of both the inhibitors occupy same place, and interact with the same amino acid residues in an identical manner (Fig. S4). Kinetic study performed by Bouhss *et al.* suggested that despite differences in its chirality, both isomeric forms of the glutamic acid analogues possessed similar affinity for the active site residues (Bouhss *et al.*, 1999).

Furthermore, compounds viz. **17k, 17d, 38** and **17c** showed higher docking scores (> -8.5). **17k**, a top ranked compound based on docking score was com-

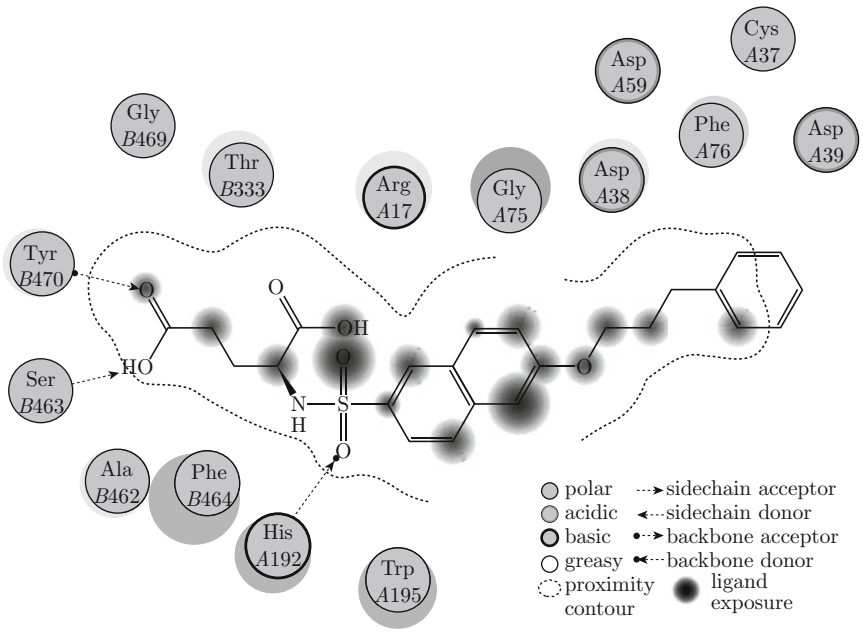

Fig. 5 2D interaction map of compound **17k** at the active site of *Mtb*-MurD ligase. Amino acid residues are indicated using three-letters code. Only some of them are shown for simplicity. Arrow indicates the hydrogen bonding interaction with the enzyme.

prised of un-substituted aromatic ring separated from naphthalene moiety with an aliphatic chain of three carbons. These conformational aspects had better molecular orientation, and thereby, molecular interactions due to large number of rotatable bonds lead to higher docking scores. The rest of the compounds viz. **17d, 38** and **17c** contain an aliphatic side chain of four or more carbons forming a hydrophobic moiety, and also additional hydrogen bonding with Arg17. All these observations are important to understand the binding affinity towards *Mtb*-MurD.

Compounds viz. **17n, 17m**, **17l** and **17o** showed reasonably lesser docking scores as compared to compounds **17k, 17d, 38** and **17c** respectively. It might be probably due to the presence of a substituted aromatic ring separated from naphthalene moiety with only one carbon, thereby restricting the movement of aromatic ring due to less number of rotatable bonds. This may be affecting the conformational orientation and interaction of the compounds in the active site cavity of the *Mtb*-MurD model.

In case of phosphinate series, compounds which are having less residual activity **12g, 12c, 12f, 13i, 12e, 12b, 13h, 12d** and **13g** showed good docking scores (> -7.0). Most of the compounds from both the series were making expected hydrogen bonding interactions with the residues Arg382, Ser463 and Tyr470 respectively, which showed that glutamic acid moiety of the ligand is responsible for the hydrogen bonding interactions in the (*Mtb*-MurD)-ligand complexes.

Compounds **16c, 17m**, **18** and **31** from naphthalene-$N-$sulfonyl-D-glutamic acid series and **23** from phosphinate series did not show any of the expected hydrogen bonding interactions. The compounds **23, 16c** and **18** are devoid of glutamic acid moiety. Therefore, absence of hydrogen bonding interaction was generally expected. Compound **31** and **17m** contain methyl substitution at sulfonyl group and disubstituted benzyl group respectively, which might be causing interference in proper orientation of these compounds at the active site cavity of *Mtb*-MurD ligase.

In addition to hydrogen bonding interactions, residues Gly75, Phe76, Trp195, Ala462 and Phe464 are observed to form van der Waals interactions with the ligand (**17k**) and was depicted in Fig. 5 as two dimensional (2D) (*Mtb*-MurD)-**17k** interaction map. Despite of being surrounded by aromatic residues, $\pi - \pi$ stacking was not observed in the active site of *Mtb*-MurD ligase in complex with **17k**.

The docking analysis of the studied compounds was generally emphasized the orientation of these compounds in the active site of the *Mtb*-MurD model. The hydrogen bonding interactions with residues Ser463, Tyr470, and His192 or Arg382 were observed to stabilize such preferred orientation of ligand in the active site. In addition, contribution of hydrophobic interactions is important due to the presence of phenyl/naphthyl moiety in the compounds. However, no significant $\pi - \pi$ stacking interactions were observed between (*Mtb*-MurD)-ligand complexes. In general, hydrogen bonding as well as the van der Waals interactions between *Mtb*-MurD with the ligand seems to dom-

inate for the ligase inhibition.

4 Conclusions

Mtb-MurD ligase is a potential drug target for the inhibition of growth of mycobacterium and hence for the treatment of TB. To understand the binding mode analysis and structural features of the enzyme, homology modeling of *Mtb*-MurD ligase was performed, as the crystal structure of this enzyme is not available till date. The overall structure quality, dihedral angle distribution and atomic interactions were found to be reasonably good for our developed *Mtb*-MurD ligase model.

MD simulations also supported the stability of the predicted *Mtb*-MurD model, as potential energy and RMSD remained stable throughout the simulation time. MD shows that three hydrogen bonds are involved to stabilize the enzyme-ligand complexes. Such predictions are also supported by the docking study, where three residues viz Ser463, Tyr470, and His192 or Arg382 are known to make hydrogen bonding interactions with the ligand. *Mtb*-MurD ligase structure remained stable as RMSF of Cα atom was found not to exceed above 0.2 nm except for few regions of protein structure throughout 4 ns MD simulations.

Docking study revealed the binding mode of *E.coli*-MurD ligase inhibitors in the homology model of *Mtb*-MurD ligase. Most of the compounds are making expected hydrogen bonding interactions with Arg382, Ser463 and Tyr470 residues, which showed that glutamic acid moiety present in most of the MurD inhibitors is quite responsible for the hydrogen bonding interactions. In addition, His192 is also an important residue for protein-ligand interaction.

Docking results also suggested that compounds containing an unsubstituted aromatic ring separated from the naphthalene ring with the aliphatic chain of three or more carbon atoms are potent inhibitors of *Mtb*-MurD ligase, as they get more flexibility at the active site cavity to make possible interactions. Glutamic acid moiety of inhibitors is observed to play an important role for making hydrogen bond interactions with the active site residues and stabilizing protein-ligand complexes. Also binding modes of isomeric form (D and L-glutamic acid) of inhibitors are found to be similar, which signifies that both the isomeric inhibitors are equally efficient for inhibiting *Mtb*-MurD ligase. All the cumulative information regarding the structure of *Mtb*-MurB ligase, MD simulations and docking study provided a significant support for the rational design of lead compounds against TB chemotherapy.

Electronic Supplementary Material

Supplementary material is available in the online version of this article at http://dx.doi.org/10.1007/s12539-012-0133-x and is accessible for authorized users.

Acknowledgements Authors are thankful to Department of Petrochemicals, Government of India for financial support.

References

[1] Anishetty, S., Pulimi, M., Pennathur, G. 2005. Potential drug targets in Mycobacterium tuberculosis through metabolic pathway analysis. Comput Biol Chem 29, 368–378.

[2] Bernstein, F.C., Koetzle, T.F., Williams, G.J., Meyer, E.F. Jr, Brice, M.D., Rodgers, J.R., Kennard, O., Shimanouchi, T., Tasumi, M. 1977. The protein data bank: A computer-based archival file for macromolecular structures. J Mol Biol 112, 535–542.

[3] Bertrand, J.A., Auger, G., Martin, L. 1999. Determination of the MurD mechanism through crystallographic analysis of enzyme complexes1. J Mol Biol 289, 579–590.

[4] Boeckmann, B., Bairoch, A., Apweiler, R., Blatter, M.C., Estreicher, A., Gasteiger, E., Martin, M.J., Michoud, K., O'Donovan, C., Phan, I., Pilbout, S., Schneider, M. 2003. The SWISS-PROT protein knowledgebase and its supplement TrEMBL in 2003. Nucleic Acids Res 31, 365–370.

[5] Bouhss, A., Dementin, S., Parquet, C., Mengin-Lecreulx, D., Bertrand, J.A., Le Beller, D., Dideberg, O., van Heijenoort, J., Blanot, D. 1999. Role of the ortholog and paralog amino acid invariants in the active site of the UDP-MurNAc-L-alanine: D-glutamate ligase (MurD). Biochemistry 38, 12240–12247.

[6] Chenna, R., Sugawara, H., Koike, T., Lopez, R., Gibson, T.J., Higgins, D.G., Thompson, J.D. 2003. Multiple sequence alignment with the Clustal series of programs. Nucleic Acids Res 31, 3497–3500.

[7] Cole, S.T., Brosch, R., Parkhill, J., Garnier, T., Churcher, C., Harris, D., Gordon, S.V., Eiglmeier, K., Gas, S., Barry, C.E. 3rd, Tekaia, F., Badcock, K., Basham, D., Brown, D., Chillingworth, T., Connor, R., Davies, R., Devlin, K., Feltwell, T., Gentles, S., Hamlin, N., Holroyd, S., Hornsby, T., Jagels, K., Krogh, A., McLean, J., Moule, S., Murphy, L., Oliver, K., Osborne, J., Quail, M.A., Rajandream, M.A., Rogers, J., Rutter, S., Seeger, K., Skelton, J., Squares, R., Squares, S., Sulston, J.E., Taylor, K., Whitehead, S., Barrell, B.G. 1998. Deciphering the biology of Mycobacterium tuberculosis from the complete genome sequence. Nature 393, 537–544.

[8] Crick, D.C., Mahapatra, S., Brennan, P.J. 2001. Biosynthesis of the arabinogalactan-peptidoglycan complex of Mycobacterium tuberculosis. Glycobiology 11, 107–118.

[9] Eldridge, M.D., Murray, C.W., Auton, T.R., Paolini, G.V., Mee, R.P. 1997. Empirical scoring functions: I.

The development of a fast empirical scoring function to estimate the binding affinity of ligands in receptor complexes. J Comput Aid Mol Des 11, 425–445.

[10] El Zoeiby, A., Sanschagrin, F., Levesque, R.C. 2003. Structure and function of the Mur enzymes: development of novel inhibitors. Mol Microbiol 47, 1–12.

[11] Emanuele, J.J. Jr., Jin, H., Yanchunas, J. Jr. 1997. Evaluation of the kinetic mechanism of Escherichia coli uridine diphosphate-N-acetylmuramate: L-alanine ligase. Biochemistry 36, 7264–7271.

[12] Falk, P.J., Ervin, K.M., Volk, K.S. 1996. Biochemical evidence for the formation of a covalent acyl-phosphate linkage between UDP-N-acetylmuramate and ATP in the *Escherichia coli* UDP-N-acetylmuramate: L-alanine ligase-catalyzed reaction. Biochemistry 35, 1417–1422.

[13] Friesner, R.A., Banks, J.L., Murphy, R.B., Halgren, T.A., Klicic, J.J., Mainz, D.T., Repasky, M.P., Knoll, E.H., Shelley, M., Perry, J.K., Shaw, D.E., Francis, P., Shenkin, P.S. 2004. Glide: A new approach for rapid, accurate docking and scoring. 1. Method and assessment of docking accuracy. J Med Chem 47, 1739–1749.

[14] Humljan, J., Kotnik, M., Contreras-Martel, C., Blanot, D., Urleb, U., Dessen, A., Solmajer, T., Gobec, S. 2008. Novel naphthalene-N-sulfonyl-d-glutamic acid derivatives as inhibitors of MurD, a key peptidoglycan biosynthesis enzyme. J Med Chem 51, 7486–7494.

[15] Khasnobis, S., Escuyer, V.E., Chatterjee, D. 2002. Emerging therapeutic targets in tuberculosis: Postgenomic era. Expert Opin Ther Tar 6, 21–40.

[16] Kotnik, M., Humljan, J., Contreras-Martel, C., Oblak, M., Kristan, K., Hervé, M., Blanot, D., Urleb, U., Gobec, S., Dessen, A., Solmajer, T. 2007. Structural and functional characterization of enantiomeric glutamic acid derivatives as potential transition state analogue inhibitors of MurD ligase. J Mol Biol 370, 107–115.

[17] Kumar, V., Saravanan, P., Arvind, A., Mohan, C.G. 2010. Identification of hotspot regions of MurB oxidoreductase enzyme using homology modeling, molecular dynamics and molecular docking techniques. J Mol Mod 17, 939–953.

[18] Lindahl, E., Hess, B., van der Spoel, D. 2001. GROMACS 3.0: A package for molecular simulation and trajectory analysis. J Mol Mod 7, 306–317.

[19] Martí-Renom, M.A., Stuart, A.C., Fiser, A., Sánchez, R., Melo, F., Sali, A. 2000. Comparative protein structure modeling of genes and genomes. Annu Rev Biophys Biomol Struct 29, 291–325.

[20] Murray, C.J., Styblo, K., Rouillon, A. 1990. Tuberculosis in developing countries: Burden, intervention and cost. Bull Int Union Tuberc Lung Dis 65, 6–24.

[21] Neubig, R.R., Spedding, M., kenakin, T., Christopoulos, A. 2003. International union of pharmacology committee on receptor nomenclature and drug classification. XXXVIII. Update on terms and symbols in quantitative pharmacology. Pharmacol Rev 55, 597–606.

[22] Parish, T., Stoker, N.G. 1999. Mycobacteria: Bugs and bugbears (Two steps forward and one step back). Mol Biotechnol 13, 191–200.

[23] Raviglione, M.C., Pio, A. 2002. Evolution of WHO policies for tuberculosis control, 1948–2001. Lancet 359, 775–780.

[24] Spigelman, M.K. 2007. New tuberculosis therapeutics: A growing pipeline. J Infect Dis 196, 28–34.

[25] Štrancar, K., Blanot, D., Gobec, S. 2006. Design, synthesis and structure–activity relationships of new phosphinate inhibitors of MurD. Bio Med Chem Lett 16, 343–348.

[26] White, T.A., Kell, D.B. 2004. Comparative genomic assessment of novel broad-spectrum targets for antibacterial drugs. Comp Funct Genomics 5, 304–327.

[27] Zhang, R., Ou, H.Y., Zhang, C.T. 2004. DEG: A database of essential genes. Nucleic Acids Res 32, D271.